Diffusion of Large Two-Dimensional Ag Clusters on Ag(100)

J.-M. Wen, S.-L. Chang, J. W. Burnett,* J. W. Evans, and P. A. Thiel
Departments of Chemistry and Mathematics and Ames Laboratory, Iowa State University, Ames, Iowa 50011
(Received 21 January 1994)

Scanning tunneling microscopy shows that large two-dimensional Ag clusters on Ag(100) can diffuse. The value of the diffusion coefficient at room temperature is of order 10^{-17} cm^2 s^{-1} and varies little, if at all, with cluster size in the range studied, 100 to 720 atoms per cluster. This weak variation rules out periphery diffusion as the main mechanism of cluster diffusion, suggesting instead two-dimensional evaporation-condensation. This conclusion is compatible with the energetics of atomic-scale events within the cluster and with the dissolution of small clusters observed at low coverages.

PACS numbers: 68.35.Fx, 61.16.Ch, 66.30.Fq, 68.60.-p

Diffusion of metal clusters can be important in metal film growth kinetics [1] and in coarsening processes, such as sintering. While experimental and theoretical studies over the past 20 years have led to the general expectation that small, two-dimensional (2D) metal clusters can undergo diffusion on metal substrates [2], large 2D clusters are not generally expected to diffuse. However, in this paper we report that *very large* two-dimensional Ag clusters (containing ca 10^2 to 10^3 atoms, N) undergo measurable diffusion on a Ag(100) surface. We also present estimates of the diffusion coefficient D of large Ag clusters and analyze the variation of D with N. This, together with analysis of atomic-scale energetics, allows us to infer the mechanism by which diffusion occurs.

Previous experimental and theoretical work has shown that the mobility of small clusters ($N < 20$) decreases with increasing size, although some sizes display anomalously high mobilities [3–7]. The mechanism of diffusion usually is proposed to be short-range motion of a single atom away from the periphery, followed by regrouping of the cluster around the departed atom [6,8], with some evidence for concerted gliding also available [5]. For larger 3D metal clusters, there exists a body of work concerning diffusion on nonmetallic substrates such as alkali halides [9–11], and here it has been shown that lattice mismatch can be important in determining diffusion characteristics [9,12]. However, for large 2D metal clusters ($N > 50$) on *metallic* substrates, we know of no previous experimental observations of diffusion.

Our experimental data are acquired with an Omicron scanning tunneling microscope (STM) housed in an ultrahigh vacuum chamber, with base pressure of 6×10^{-11} to 3×10^{-10} Torr. The microscope can routinely resolve the atomic-scale unit cells within the (100) terraces. Silver is deposited on a Ag(100) crystal from a resistively heated liquid-nitrogen-shrouded source. Evaporation of submonolayer coverages with the crystal at room temperature results in compact two-dimensional Ag structures, such as islands, whose position, size, and shape is followed quantitatively as a function of time over a period of several h. The interval between measurements is typically 10 to 15 min. In order to establish fixed points of spatial reference, we include in the images a step edge containing an impurity; the step edge is then assumed to be pinned in the vicinity of the impurity [13].

The Ag islands can be perturbed by the tunneling tip. For instance, efforts to obtain atomic-scale resolution on small islands ($N < 30$) invariably perturb the island. Therefore, we limit examination to islands of $N \geq 100$; further, we sacrifice spatial resolution to minimize perturbation. The images are typically obtained in the constant-current mode, with 1.0–1.1 V bias voltage and 3.0–3.4 nA tunneling current. We further examine the effect of different raster frequencies. Between the minimum raster rate accessible (one image per 10–15 min interval) and the maximum rate (ca 7 images per interval), we find no effect on the quantitative results reported here. This suggests that the tip does not induce the motion of the clusters.

We begin with the basic experimental observation, illustrated in Fig. 1. The bright spots in the image are Ag clusters in the middle of a large terrace; the larger ill-defined white shape toward the upper right is a spot of contamination, probably carbon; the diagonal line which contains it is a monatomic step edge. The Ag islands adopt an approximately square shape, although irregularities such as rounded corners and crooked edges are common. The Ag clusters in Fig. 1 range in size from 100 to 800 atoms (830 to 6640 Å^2). Comparison of Fig. 1(a) with 1(b) clearly shows that the Ag clusters have moved in the interval between images, in this case 5.7 h. The trajectories of two differently sized clusters are illustrated in Figs. 2(a)–2(b). Over a period of several h, the net displacement of the clusters is on the order of 10^2 Å. Qualitatively, the trajectories appear to be random (diffusive).

Diffusion coefficients are extracted from trajectories such as those of Fig. 2. Trajectories are analyzed only for those intervals where the clusters remain constant in size, to within ±15%, and where the clusters remain at least 300 Å (and more typically, 500–600 Å) away from a step edge. Figure 3 shows the quantity $\langle d^2/t \rangle$, where d is the displacement between the cluster's center-of-mass location, as a function of the mean time interval between ob-

0031-9007/94/73(19)/2591(4)$06.00

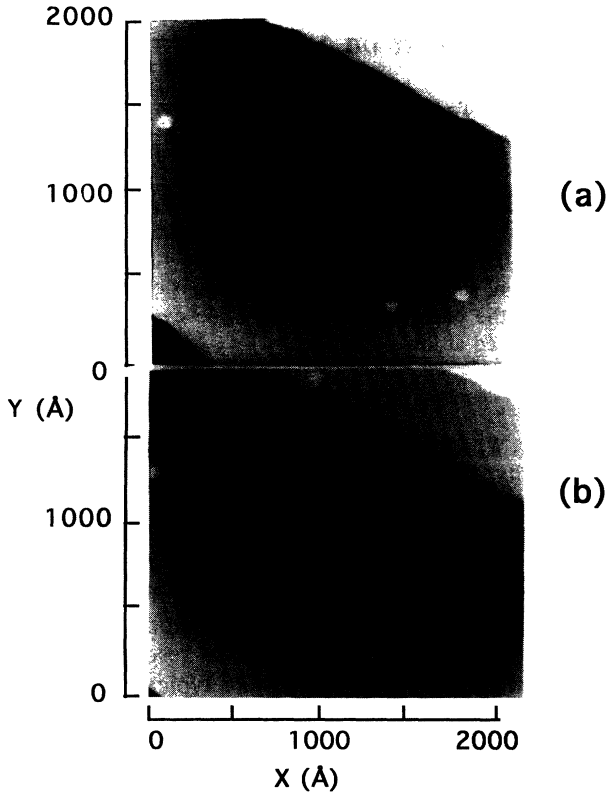

FIG. 1. STM images obtained following deposition of 0.007 monolayers (ML) Ag on Ag(100) at room temperature. The deposition rate is 4×10^{-3} ML/s. (a) $t = 0$ h. (b) $t = 5.7$ h. Contamination at step edge is most apparent in (b).

servations, $\langle t \rangle$, for two differently sized clusters. The diffusion coefficient D is then defined as $\lim_{\langle t \rangle \to \infty} D(t)$, where $D(t) = \frac{1}{4}\langle d^2/t \rangle$. Thus, D is extracted from the value of the plateau in $\langle d^2/t \rangle$ at long $\langle t \rangle$. The fact that $\langle d^2/t \rangle$ does reach a plateau demonstrates that motion of the clusters, at long $\langle t \rangle$, is diffusive. However, the value of $\langle d^2/t \rangle$ *always* shows a sharp decline at small values of $\langle t \rangle$. This signifies a slight tendency for clusters to move opposite the direction of recent motion—a "back correlation." Such an effect has not been observed in previous experimental studies, although it has been observed in simulations of cluster diffusion, where it was associated with the requirement of cluster "connectivity" [14].

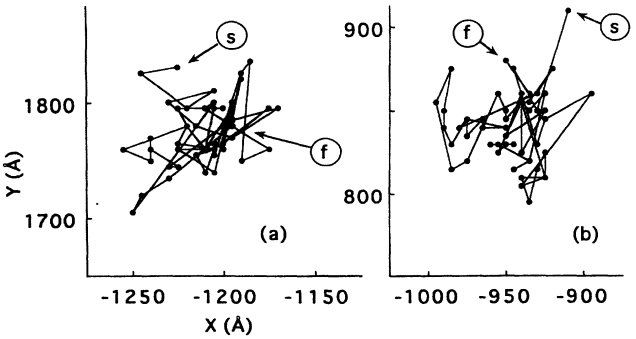

FIG. 2. Trajectories for two differently sized clusters. The starting and final locations are indicated by s and f, respectively. (a) $N = 110$. (b) $N = 290$.

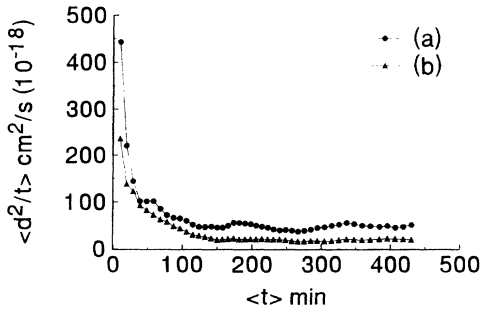

FIG. 3. $\langle d^2/t \rangle$ vs $\langle t \rangle$, corresponding to the trajectories of Fig. 2. (a) $N = 110$. (b) $N = 290$.

Figure 4 shows the value of D as a function of cluster size, with the experimental data represented by crosses. For $100 \leq N \leq 720$, D varies from 5.3×10^{-18} to 2.7×10^{-17} cm^2 s^{-1}. However, there is little—if any—systematic variation of D with N (a factor of 2 at most).

It is worth considering the possibility that adsorption of background gases plays some role in cluster diffusion, especially in light of the work by Cooper *et al.*, showing that atmospheric contamination can strongly influence mass transport on Au [15,16]. While adsorption of background gases can never be ruled out entirely, there are several factors which make the role of such contaminants unlikely here. First, in these experiments no static contaminants are imaged with the STM on the Ag(100) terraces; as noted above, the unit cells of the clean metal can be routinely resolved, and one would expect contamination at the surface to perturb such an image significantly—as it does at

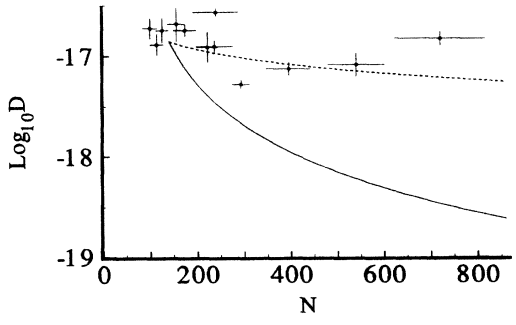

FIG. 4. Diffusion coefficient at room temperature as a function of cluster size. Each cross represents experimental error estimated for each data point, not a statistical variance. Solid line shows scaling relationship $D \sim N^{-1.75}$ [18], arbitrarily placed to coincide with experimental values at $N \approx 10^2$. Dashed line shows $D \sim N^{-0.5}$ as discussed in text, placed similarly.

the steps. Second, Ag is inert toward most common gases at room temperature. Third, when the edges of the large clusters are imaged, they appear frizzy (*vide infra*); in our experience, this frizziness is only obtained when foreign material is absent from the step edge [17]. Finally, the value of D we measure on an obviously contaminated terrace is drastically lower than that which we report here.

We consider two main, nonexclusive mechanisms which could facilitate cluster diffusion. The first is periphery diffusion (PD), i.e., atomic motion along the cluster periphery. The second is two-dimensional (2D) evaporation-condensation (EC), in which atoms leave and reattach to cluster edges. In the EC mechanism, clusters are in a dynamic quasiequilibrium with a dilute 2D gas of Ag atoms on the terrace. It might be anticipated that the PD mechanism would always dominate, since barriers for atoms to move along the edge are intuitively expected to be much lower than for atoms to leave (evaporate from) the cluster. Ultimately, we shall show that this is a false expectation. First, however, let us assess which mechanism is most compatible with the experimental data.

Comparison of the EC and PD models with experimental data hinges upon predictions of D as a function of N. Specifically, we seek the exponent α, which describes $D \propto N^{-\alpha}$, for large N. For PD, Monte Carlo simulations are available which yield exact results, showing $\alpha \approx 1.5$ to 2 [14,18,19]. Two of the simulations have even specifically modeled metal-on-metal systems, $Ag_N/Ag(100)$ and $Rh_N/Rh(100)$, and both yield $\alpha \approx 1.75$ [18,19]. The strong variation of D with N given by this value of α is shown by the solid line in Fig. 4; it is clearly incompatible with the experimental results.

Unfortunately, there are no corresponding simulations available for the EC mechanism. In order to assess $D(N)$ for EC, we can write [14,20]

$$D \propto \langle H_N \rangle \langle \delta d_{\mathrm{CM}^2} \rangle . \tag{1}$$

For EC, $\delta d_{\mathrm{CM}} = 1/\sqrt{N}$ is the center-of-mass (CM) displacement of the cluster in lattice constants, per edge-atom removal, and $\langle H_N \rangle$ is the total evaporation (or condensation) rate. If $\langle H_N \rangle \propto N^{0.5}$ for compact clusters, then $D \propto N^{-0.5}$. This relatively weak dependence on N is shown by the dashed line in Fig. 4 and is roughly consistent with the experimental data. Note that for PD, $\delta d_{\mathrm{CM}} = 1/N$ per edge-atom hop in Eq. (1), and $\langle H_N \rangle$ is the total rate of edge hops contributing to cluster diffusion [20], again assumed to vary as $N^{0.5}$. Hence $D \propto N^{-1.5}$ for the PD mechanism from Eq. (1), in reasonable agreement with the Monte Carlo simulations. The main point, overall, is that the experimental data favor the EC mechanism, based upon predictions of $D(N)$ for both models.

In order to understand further the diffusion mechanisms and their ramifications, consider the atomic-scale processes which may occur at the edge of a cluster. Starting with the PD processes, they are shown by Fig. 5 *a* through *c'*. The activation energies calculated from the embedded atom method (EAM) indicate that energy barriers are about equal for the processes represented by Fig. 5 *b* and *b'*. The same is true for Fig. 5 *c* and *c'* [19]. Using the EAM-based barriers, relative rates are next fastest by Fig. 5 *b*, *b'* (ca $10^{-3.5}$ s), and slowest by Fig. 5 *c*, *c'* (ca 10^2 s) [19]. Experimental data support the idea that one or more of the "fast" processes does occur, on a time scale which is at least shorter than the imaging process: with atomic-scale resolution, edges of large terraces, and large islands appear frizzy in our STM images. In studies of other metal surfaces, this phenomenon has been attributed to the escape of atoms from kink sites (Fig. 5 *b*) [21,22].

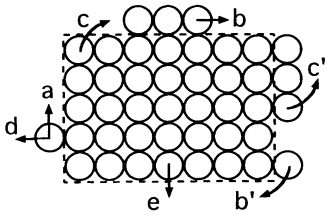

FIG. 5. Schematic representation of atomic-scale processes: Rapid single-atom edge-diffusion (*a*); less-rapid escape from kinds (*b*) and corner-rounding (*b'*); slow core breakup (*c*), climbing onto a fresh edge (*c'*), ore evaporation (*d*); core breakup via (e) is effectively inoperative at 300 K. The dashed line shows the cluster "core."

Thus, one might expect that the fast, easy processes of Fig. 5 *a*, *b*, and *b'* dominate cluster diffusion, at least under the PD mechanism. However, this is not true because of a "core breakup" requirement. At any moment in time, the cluster can be conceptually divided into a rough edge zone, and an inner, rectangular core. The core is outlined in Fig. 5. If atomic-scale motion is limited to the edge zone, i.e., if only the fast processes occur, the inner core cannot move. With such a limitation, only slight displacements in the center of mass take place, due to fluctuations in atom distributions along the edges, and the cluster is effectively "tethered" by the core. Long-range motion, such as we observe, requires that atoms exchange with the core itself. Hence, in PD, long-range diffusion is dominated by the slow processes of Fig. 5 *c*, wherein atoms leave the core.

Proof lies in EAM studies which show that, when clusters are constrained to diffuse via PD, i.e., when detachment is not allowed, core breakup is rate determining [18,19]. More specifically, Voter's EAM-based simulation of large Ag cluster diffusion via PD [19] yields a variation of D with N which can be fitted by

$$D \approx 0.03 N^{-1.75} \exp[(-0.82\ \mathrm{eV})/k_B T]\ \mathrm{cm^2\,s^{-1}}. \tag{2}$$

The barrier of 0.82 eV in Eq. (2) corresponds precisely to the EAM barrier for core breakup. Interestingly, Eq. (2) yields a value of $D \approx 1.6 \times 10^{-19}\ \mathrm{cm^2\,s^{-1}}$ for $N = 100$

at 300 K, which is 2 orders of magnitude below the experimental value. However, the experimental value of D can be recovered by retaining roughly the same barrier (*vide infra*) and prefactor in Eq. (2), but replacing the N dependence by $N^{-0.5}$, as predicted by Eq. (1) for EC. This, plus Voter's observation that clusters tend to dissociate rather than move over distances >10 Å [19], also supports EC rather than PD.

Core breakup is actually required for long-range diffusion under *both* of the mechanisms postulated here, PD and EC. The difference is that in PD, core breakup alone causes long-range diffusion, whereas in EC, core breakup must be followed by atom detachment (Fig. 5 d). In fact, EAM studies of metal systems show that the effective barrier for evaporation [23], and thus for EC, is comparable to that for core breakup [19]. Thus, if the barrier for core breakup can be surmounted, so too can that for evaporation. It follows that any intuitive expectation that PD dominates over EC, based on atomic-scale energetics, is false.

If core breakup and evaporation have comparable barriers, why then should either EC or PD prevail? The answer must lie in the weights associated with the rate-limiting events. For instance, in Eq. (1), the values of δd_{CM^2} are N^{-1} and N^{-2} for EC and PD, respectively. In other words, each evaporation even in EC triggers a much larger change in the cluster's center of mass, than does each core breakup event in PD.

There is also *direct experimental evidence that evaporation and condensation occur at cluster edges in our system.* This is most clear at low coverages (below ca 0.1 monolayer) from the long-term changes in island size: Small islands tend to disappear; large islands tend to remain constant or (occasionally) grow larger. Such changes are evident in Fig. 1. This phenomenon, known as Ostwald ripening, can occur *only* if a 2D gas is present to mediate exchange between the islands. Hence, the existence of a dilute 2D gas phase, which is required under the EC mechanism, is supported unequivocally by the experimental data.

Finally, cluster diffusion should not be regarded simply as an isolated, esoteric phenomenon; it can have important consequences for the evolution of thin film structure. The long-term coarsening of 2D homoepitaxial adlayers is traditionally regarded as being dominated by Ostwald ripening, and it is assumed also that the centers of mass of the clusters remain fixed [24]. However, cluster diffusion can lead to coalescence, a completely different channel for coarsening. In fact, we have recently begun to study coarsening over long times for Ag/Ag(100) and find that diffusion-mediated coalescence plays a major role over a wide range of conditions. This leads to a radically different view of the coarsening process, which should be important in any system where cluster diffusion is significant. Details will be reported elsewhere.

We thank A. F. Voter and R. J. Behm for stimulating and informative discussions. This work is supported by NSF Grant No. CHE-9317660. One of us (P. A. T.) also acknowledges support of a National Science Foundation Faculty Award for Women in Science and Engineering. Some equipment and all facilities are provided by the Ames Laboratory. Ames Laboratory is operated for the U.S. Department of Energy by Iowa State University under Contract No. W-7405-Eng-82.

*Present address: Department of Chemistry, University of Iowa, Iowa City, Iowa 52242-1294.

[1] J. A. Venables, G. D. T. Spiller, and M. Hanbuecken, Rep. Prog. Phys. **47**, 399 (1984), and references therein.
[2] S.-L. Chang and P. A. Thiel, CRC Crit. Rev. Sur. Chem. **3**, 239 (1994).
[3] D. W. Bassett, J. Phys. C. **9**, 2491 (1976).
[4] T. T. Tsong and R. Casanova, Phys. Rev. B **22**, 4632 (1980).
[5] H.-W. Fink and G. Ehrlich, Surf. Sci. **150**, 419 (1985).
[6] S. C. Wang and G. Ehrlich, Surf. Sci. **301**, 239 (1990).
[7] G. L. Kellogg, Appl. Surf. Sci. **67**, 134 (1993).
[8] C.-L. Liu and J. B. Adams, Surf. Sci. **268**, 73 (1992).
[9] A. Masson, J. J. Metois, and R. Kern, Surf. Sci. **27**, 463 (1971).
[10] C. R. Henry, C. Chapon, and B. Mutaftschiev, Thin Solid Films **46**, 157 (1977).
[11] C. Chapon and C. R. Henry, Surf. Sci. **106**, 152 (1981).
[12] R. Kern, A. Masson, and J. J. Metois, Surf. Sci. **27**, 483 (1971).
[13] J. S. Ozcomert *et al.*, Surf. Sci. **293**, 183 (1993).
[14] H. C. Kang, P. A. Thiel, and J. W. Evans, J. Chem. Phys. **93**, 9018 (1990).
[15] D. R. Peale and B. H. Cooper, J. Vac. Sci. Technol. A **10**, 2210 (1992).
[16] B. H. Cooper *et al.*, Mater. Res. Soc. Symp. Proc. **280**, 37 (1993).
[17] S.-L. Chang *et al.* (to be published).
[18] A. F. Voter, Phys. Rev. B **34**, 6819 (1986).
[19] A. F. Voter, SPIE Modeling of Optical Thin Films **821**, 214 (1987).
[20] An exact treatment for PD replaces Eq. (1) with $D = C_N\langle T_N\rangle\langle\delta d_{CM^2}\rangle$, where $\delta d_{CM} = 1/N$, $\langle T_N\rangle$ is the total hop rate, and $C_N < 1$ measures the back correlation in the walk [14]. Microscopically, $C_N \ll 1$ since most hops are ineffective. Another perspective considers many-atom effective events, where core breakup is quickly followed by, e.g., removal of an entire edge. Here $\delta d_{CM}(\text{eff}) = 1$ and the effective event rate decreases strongly with N for PD (but not for EC).
[21] M. Giesen-Seibert *et al.*, Phys. Rev. Lett. **71**, 3521 (1993).
[22] L. Kuipers, M. S. Hoogeman, and J. W. M. Frenken, Phys. Rev. Lett. **71**, 3517 (1993).
[23] The effective barrier for evaporation of a corner core atom is the maximum of the barriers for the individual steps (core breakup, Fig. 5 *c*, and detachment from a straight [011] edge, Fig. 5 *d*) and the collective barrier $E_d + \Delta E$, where E_d is the isolated atom diffusion barrier, and ΔE is the corner atom binding energy.
[24] H.-J. Ernst, F. Fabre, and J. Lapujoulade, Phys. Rev. Lett. **69**, 458 (1992).

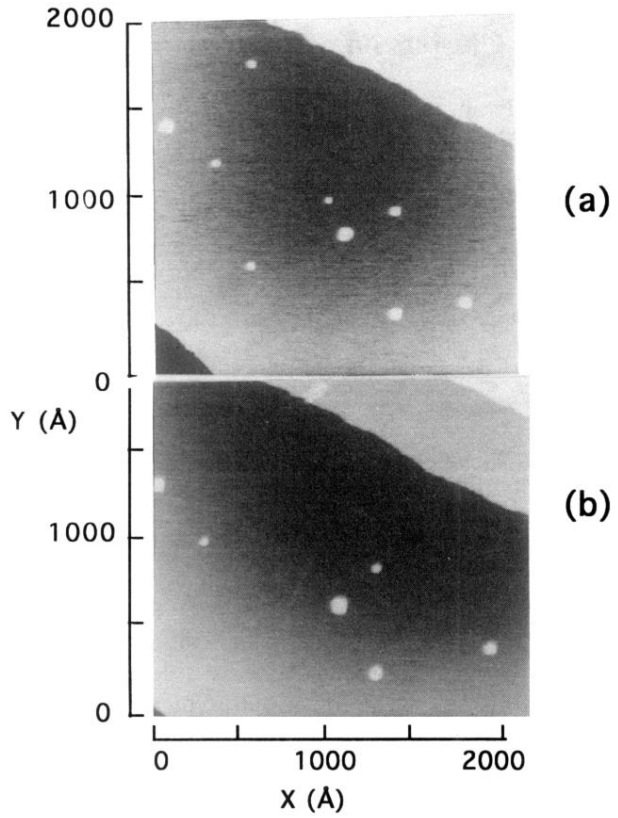

FIG. 1. STM images obtained following deposition of 0.007 monolayers (ML) Ag on Ag(100) at room temperature. The deposition rate is 4×10^{-3} ML/s. (a) $t = 0$ h. (b) $t = 5.7$ h. Contamination at step edge is most apparent in (b).